Title
Using airborne lidar to predict Leaf Area Index in cottonwood trees and refine riparian water-use estimates

Journal
Journal of arid environments, 72(1)

ISSN
0140-1963

Authors
Farid, A
Goodrich, DC
Bryant, R
et al.

Publication Date
2008

DOI
10.1016/j.jaridenv.2007.04.010

ELSEVIER

Journal of Arid Environments 72 (2008) 1–15

Journal of Arid Environments

www.elsevier.com/locate/jaridenv

Review

Using airborne lidar to predict Leaf Area Index in cottonwood trees and refine riparian water-use estimates

A. Farid[a,*], D.C. Goodrich[b], R. Bryant[b], S. Sorooshian[c]

[a]*Department of Hydrology and Water Resources, University of Arizona, Tucson, AZ 85721, USA*
[b]*USDA-ARS-SWRC, Southwest Watershed Research Center, Tucson, AZ, USA*
[c]*Department of Civil and Environmental Engineering, University of California, Irvine, CA, USA*

Received 26 April 2006; received in revised form 12 March 2007; accepted 24 April 2007
Available online 6 June 2007

Abstract

Estimation of riparian forest structural attributes, such as the Leaf Area Index (LAI), is an important step in identifying the amount of water use in riparian forest areas. In this study, small-footprint lidar data were used to estimate biophysical properties of young, mature, and old cottonwood trees in the Upper San Pedro River Basin, Arizona, USA. Canopy height and maximum and mean laser heights were derived for the cottonwood trees from lidar data. Linear regression models were used to develop equations relating lidar height metrics with corresponding field-measured LAI for each age class of cottonwoods. Four metrics (tree height, height of median energy, ground return ratio, and canopy return ratio) were derived by synthetically constructing a large-footprint lidar waveform from small-footprint lidar data which were compared to ground-based high-resolution Intelligent Laser Ranging and Imaging System (ILRIS) scanner images. These four metrics were incorporated into a stepwise regression procedure to predict field-derived LAI for different age classes of cottonwoods. This research applied the Penman–Monteith model to estimate transpiration of the cottonwoods using lidar-derived canopy metrics. These transpiration estimates compared very well to ground-based sap flux transpiration estimates indicating lidar-derived LAI can be used to improve riparian cottonwood water-use estimates.

Keywords: Cottonwood; Leaf Area Index; Lidar; Riparian; San Pedro River Basin

Contents

*Corresponding author. Tel.: +1 520 891 0735; fax: +1 520 626 4479.
E-mail address: farid@hwr.arizona.edu (A. Farid).

0140-1963/$ - see front matter © 2007 Elsevier Ltd. All rights reserved.
doi:10.1016/j.jaridenv.2007.04.010

1. Introduction

Vegetation patterns and associated canopy structure influence landscape functions such as water use, biomass production, and energy cycles. The properties of vegetation and canopy must be quantified in order to understand their roles in landscapes and before management plans can be developed for the purpose of conserving natural resources. In arid and semi-arid regions, with high potential evaporative demand, the presence of perennial flow and verdant riparian corridors can constitute a major source of water use (net loss) in overall basin water budgets (US Dept. of Interior, 2006). The net loss of basin water resources from riparian evaporation and transpiration is a critical boundary condition for regional groundwater models, which is necessary for overall basin water management. However, basin-level riparian water use is difficult to estimate with standard micro-meteorological techniques due to the often narrow, non-uniform corridors, which violate the necessary fetch requirements of many of these systems (Goodrich et al., 2000). The narrow, non-uniform nature of typical riparian corridors also makes rapid measurement of critical canopy parameters for riparian evapotranspiration estimates, such as Leaf Area Index (LAI), difficult and time consuming. Remote sensing offers approaches to overcome some of these limitations and uncertainties. In particular, multi-return airborne lidar can provide the capability to identify riparian tree species (Farid et al., 2006a) and age and canopy characteristics (Farid et al., 2006b).

Recent progress in three-dimensional forest characterization at the stand level mainly includes digital stereophotogrammetry, synthetic aperture radar, and lidar (light detecting and ranging). Lidar is a technique in which light at high frequencies, typically in the infrared wavelengths, is used to measure the range between a sensor and a target, based on the round trip travel time between source and target. Airborne Laser Scanning is a measurement system in which pulses of light (most commonly produced by a laser) are emitted from an instrument mounted in an aircraft and directed to the ground in a scanning pattern. This method of recording the travel time of the returning pulse is referred to as pulse ranging (Wehr and Lohr, 1999). The type of information collected from this returning pulse distinguishes two broad categories of lidar sensors: discrete-return (small-footprint) lidar devices and full-waveform (large-footprint) recording devices. Discrete-return systems typically allow for one (e.g., first or last), two (e.g., first and last), or a few (e.g., five) returns to be recorded for each pulse during flight. Conversely, a full-waveform lidar system senses and records the amount of energy returned to the sensor for a series of equal time intervals. The number of recording intervals determines the level of detail present in a laser footprint. For forested environments, the result is a waveform indicative of the forest structure (i.e., from the top of the canopy, through the crown volume and understory layer, and finally to the ground surface). The footprint for most discrete-return systems is on the order of 0.2–0.9 m. For full-waveform systems, the footprint size may vary from 8 to 70 m (Means et al., 1999).

Previous studies model full-waveform characteristics for simple, unvegetated terrain (Gardner, 1992), and for one-dimensional surfaces (Abshire et al., 1994).

Additionally, Blair and Hofton (1999) demonstrated that vertical distribution of the discrete-return data is closely related to the full-waveforms recorded by waveform-recording devices when certain conditions are met, the most important being a high density of samples collected using a very small footprint (on the order of 25 cm).

The foundations of lidar forest measurements lie with photogrammetric techniques developed to assess tree height, canopy density, forest volume, and biomass. Airborne laser measurements were used in place of photogrammetric measurements to estimate forest heights and canopy density (Nelson et al., 1984) and forest

volume or biomass (Maclean and Krabill, 1986; Nelson et al., 1988a, b). For instance, Nelson et al. (1988b) predicted the volume and biomass of southern pine (*Pinus taeda*, *P. elliotti*, *P. echinata*, and *P. palustris*) forests using several estimates of canopy height and cover from small-footprint lidar, explaining between 53% and 65% of the variance in field measurements of these variables.

The primary objective of this research was to use a small-footprint lidar to derive various height metrics (maximum laser height, mean laser height, and canopy height) and model full-waveform characteristics in cottonwood trees in the San Pedro Riparian National Conservation Area (SPRNCA) in southeastern Arizona, USA. The SPRNCA is a globally important migratory bird route. Its cottonwood riparian forest supports a great diversity of species and is widely recognized as a regionally and globally important ecosystem (World Rivers Review, 1997). Additionally, lidar studies published at this point have shown success in several forest types with large-footprint lidar, but applications of small-footprint lidar have not progressed as far (Means, 2000), being limited mainly to measuring even-aged coniferous stands. Thus, the performance of lidar in cottonwood riparian forests remains untested and any related analytical and processing issues are yet to be identified.

The secondary objective of this study was to estimate LAI from various laser height metrics and synthetic large-footprint lidar waveform for different age classes of cottonwood trees. Additionally, this study applied the Penman–Monteith (P–M) model (Monteith and Unsworth, 1990) to estimate cottonwood transpiration using lidar-derived LAI, compared with transpiration measured by sap flow. Riparian cottonwood trees use water in proportion to their age and canopy shape (Schaeffer et al., 2000), and are especially large users of water in flood plains along rivers in semi-arid environments. More accurate quantification of riparian water use is required to manage basin water resources to maintain the economic, social, and ecological viability of these areas and ensure water for a growing human population in the basin. Cottonwoods of different age cannot be distinguished by multi-spectral methods. Because older cottonwoods exhibit a canopy that is more crowned in shape than the younger trees, differences in tree shape as a function of tree age led us to investigate the use of lidar to identify cottonwoods of different age classes and estimate LAI, both of which impact a tree's water use.

The specific objectives of this study were:

(1) Model a laser altimeter return waveform as the sum of reflections within a laser small footprint and compare the results with ground-based Intelligent Laser Ranging and Imaging System (ILRIS) scanner images in cottonwood trees.
(2) Derive maximum laser height, mean laser height, and canopy height from the small-footprint lidar data and determine how well they can estimate LAI for different age classes of cottonwoods.
(3) Derive four metrics (canopy height, height of median energy (HOME), ground return ratio (GRND), and canopy return ratio (CRND)) from synthetic lidar full waveform. These four metrics are incorporated into a stepwise regression procedure to predict field-derived LAI for different age classes of cottonwood trees.
(4) Apply the P–M model to estimate transpiration of the cottonwoods using lidar-derived LAI and compare the results with transpiration measured by sap flow techniques.

Meanwhile, the analysis presented herein focuses on isolated trees to provide a "proof of concept" of the stated objectives for this less complex case.

2. Study sites

The three study sites are located on the floodplain of the San Pedro River within the SPRNCA in southeastern Arizona, USA. The Escalante study site (31°51′N, 110°13′W; 1110 m elevation) is about 1.2 km long north to south and 1.4 km wide east to west and is relatively flat. The Escalante study site is located along an intermittent reach of the river where the groundwater depth ranged from 4.3 to 4.5 m. This study site was used to estimate LAI from various laser height metrics and synthetic large-footprint lidar waveform for different age classes of cottonwood trees. This study area is populated by young-to-old dense cottonwood stands with patches of cottonwood riparian forest located along the stream channel.

The Boquillas study site (31°69′N, 110°18′W; 1180 m elevation) is located along an intermittent reach of the river where the groundwater depth ranged from 3.1 to 3.9 m. In contrast, the Lewis Springs study site (31°33′N, 110°07′W; 1250 m elevation) is located along a perennially flowing reach of the San Pedro River where the groundwater depth ranged from 1.1 to 1.8 m. These two additional sites were used to apply the P–M model to estimate cottonwood transpiration using lidar-derived LAI, compared with transpiration measured by sap flow for individual cottonwood trees within an isolated cluster of cottonwoods. The cottonwood trees at both sites were very similar in age and size characteristics.

The overstory for these three study sites is dominated by riparian forest vegetation, such as Fremont cottonwood (*Populus fremontii*), Goodding willow (*Salix gooddingii*), and velvet mesquite (*Prosopis velutina*) woodlands. The understory consists mainly of sacaton (*Sporobolus wrightii*) grassland and tamarisk (*Tamarix chinensis*) in these three sites.

3. Data acquisition

3.1. Ground inventory data

Ground validation data were collected from April 2003 to October 2004. Three different ages of cottonwood trees were included in the field sampling—young cottonwoods (less than 15 years), mature cottonwoods (16–50 years), and old cottonwoods (greater than 50 years) (Fig. 1). Stem diameters at breast height (dbh) (diameter measured at 1.37 m above the ground) were measured with a diameter tape and recorded to the nearest mm to discriminate between young, mature, and old cottonwood patches, based on river-specific equations that relate dbh to tree age (Stromberg, 1998). Dbh values varied, from less than 25 cm for young cottonwoods, 25–90 cm for mature cottonwood stands, and greater than 90 cm for old cottonwoods.

A total of 41 cottonwood trees were used to determine LAI. Of the 41 cottonwoods, 9 old, 15 mature, and 17 young isolated trees were selected that were at least 6 m apart. A differential global positioning system (DGPS) was used to determine the location of each individual tree within sub-meter planimetric accuracy (5700 GPS, Trimble Navigation, Ltd., Sunnyvale, CA). We measured four points around each tree at the edge of the tree canopy. In addition, all tree locations were determined using 60-s static measurements with a 12-channel GPS receiver. The GPS antenna height varied between 1.8 and 3.6 m, with an average height of 2.5 m. All measurements were collected during the leaf-off season. The lack of canopy foliage and the raised antenna in the old cottonwood stands reduced the error effects of forest canopies on GPS measurements. These trees were identified in the lidar data set by matching field DGPS locations with the georeferenced lidar data.

The LAI was measured using a plant canopy analyzer (LAI 2000, Li-Cor, Inc., Lincoln, NE) in June 2003 for different age classes of cottonwoods. LAI readings were taken from the four cardinal directions around the base of each cottonwood tree by one sensor with a 90° view cap. The sensor was aligned along the canopy of

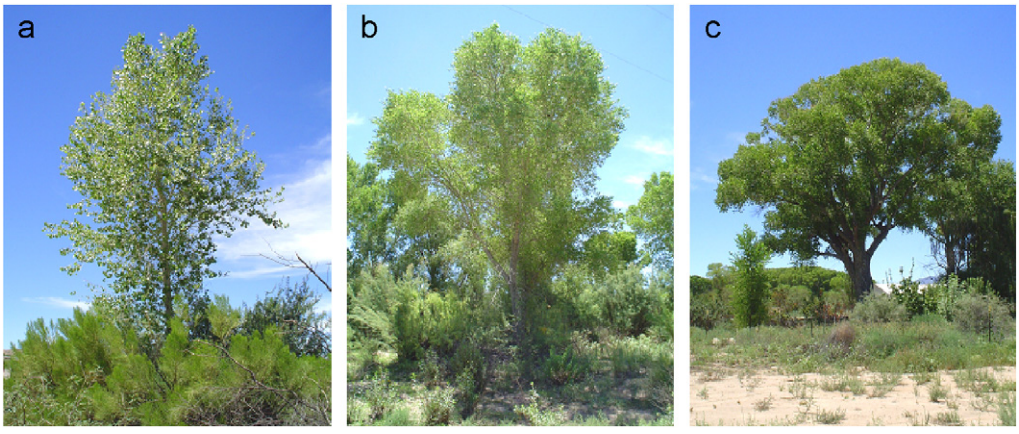

Fig. 1. Photos depicting (a) young, (b) mature, and (c) old cottonwood trees. Figure adapted from Farid et al. (2006b), with permission from the Society of American Foresters.

the tree, as well as across the canopy. Measurements were made after sunset at dusk, when the sky is still illuminated, but after the direct beam radiation leaves the canopy.

In 2006, Gazal et al. measured sap flow of four cottonwood trees within an isolated cluster at each of the two study sites (Boquillas and Lewis Springs), using constant heat flow Granier-type probes (TDP-30 and TDP-80, Dynamax, Inc., Houston, TX).

Additionally, air temperature, relative humidity, solar radiation, wind speed, and air pressure were measured at nearby meteorological towers located 3 km from the Boquillas intermittent stream site and 0.3 km from the Lewis Springs perennial stream site (Scott et al., 2000). For both perennial and intermittent stream sites, the measurements were recorded every 15 and 30 min, respectively. Stand transpiration was estimated for the period 1–11 June 2003 (DOY: 152-162), which corresponded to the timing of the lidar survey.

3.2. Lidar data sets

The Optech ALTM 1233 (Optech, Inc., Toronto, Canada) was used to survey the study site on June 6, 2003. Characteristics of the ALTM 1233 include a scanning frequency of 28 Hz, a scan angle of $\pm 20^{\circ}$, a collection mode of first and last returns, and intensity of returns from a 1064-nm laser. The ALTM 1233 was mounted on a University of Florida plane flying at 750 m above the ground at a velocity of 60 m s^{-1}. The aircraft and ALTM 1233 configuration resulted in a cross-track point spacing of 0.9 m, a forward point spacing of 2.1 m, and a footprint size of approximately 15 cm in diameter. The average ground swath width was 546 m and the entire study area was covered by four parallel flight lines. For the entire research area, 50% overlapping flight lines were used to ensure complete coverage, which generated approximately 2 million laser returns. The lidar data were processed and classified using the Optech REALM 3.0.3d software. Three data layers were produced from the classification: (1) ground last return, (2) vegetation last return and (3) vegetation first return. The ground last return data layer was a robust representation of the terrain. For this study, vegetation last and vegetation first data layers were merged into a single vegetation class. The attributes of any given laser return not only include x, y, and z coordinate data but also an intensity return value (Farid et al., 2006a).

3.2.1. Ground-based laser scanner

The ground-based laser scanner acquired for the study site on June 2004, was the Intelligent Laser Ranging and Imaging System-Three-Dimensional (ILRIS-3D, Optech, Inc., Toronto, Canada), with a vertical accuracy of 0.3 cm. The laser scanner fires a focused laser at ground targets and measures the target position based on laser travel time to the target and back to the sensor. The hit size is 1.5 cm in diameter at 50 m from the scanner, which was the approximate distance. The laser scanner collects x, y, and z relative coordinates for every 1.5 cm hit scanned for a complete three-dimensional image of the object. Distance between hits (resolution) was on average 0.2 cm. The resolution changes with distance between the target and the scanner.

Capturing an entire cottonwood tree canopy required two scans on opposite sides of the tree. If three sub-meter accuracy GPS points can be located within each scanned image, the images can easily be merged. We placed three large cardboard boxes in the foreground of each cottonwood tree that was to be scanned and then secured a piece of rebar into the ground at the corner of each box. Fig. 2 shows the boxes in the foreground of one old cottonwood tree as an example (two scans on opposite sides of the tree). These points on the ground were then georeferenced with a DGPS at a later date. The corners of the boxes where the rebar was located allowed us to locate the georeferenced points in the scanned image. Then the x, y, and z coordinates of the images were given UTM values and sea-level altitude values in meters. Unfortunately, due to our remote location which is covered by dense vegetation and the stream channel bank, only one scanned tree had georeferenced points with enough accuracy for the images to be merged accurately into a full canopy. The other trees had to be manually merged. Manually merging is a tedious process and only works if at least three common points can be located in each image that is to be merged. This limitation reduced the number of trees with fully scanned canopies to five. Therefore, of the 24 old and mature cottonwoods, three old and two mature cottonwood trees were selected. No young trees were selected because their locations were neighbored by dense vegetation, and the river bank obstructed the laser scanning beams.

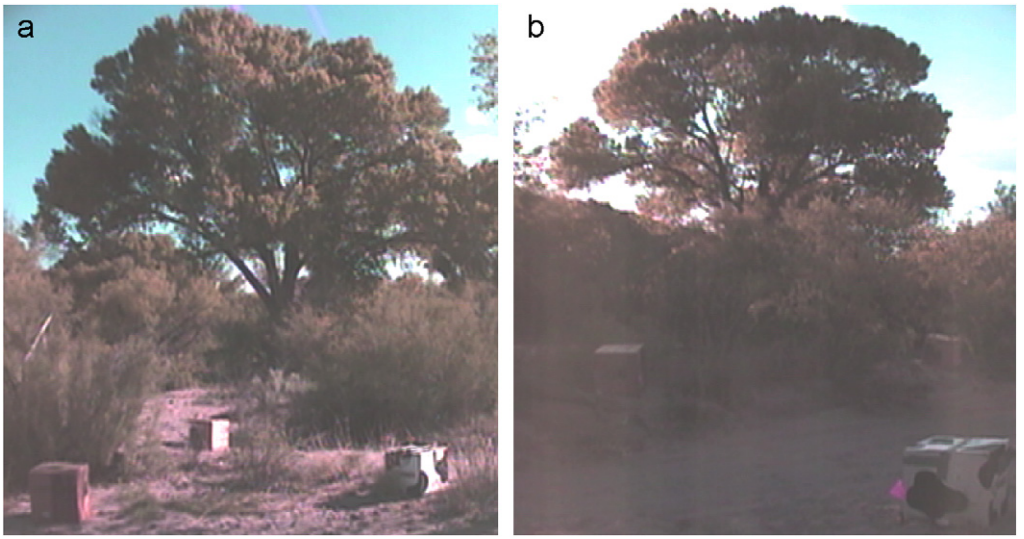

Fig. 2. Cardboard boxes in the (a) foreground and (b) back part of one of the old cottonwood trees (two scans on opposite sides the tree).

4. Analysis

This analysis will include a combination of both ground-based and airborne lidar data from 2003 and 2004.

4.1. Modeling a return waveform and comparing with ground-based laser scanner

Our model for a large-footprint lidar waveform is constructed under the assumption that the shape of any waveform represents the vertical distribution of intercepted surfaces within a small footprint. We chose the average crown width of an old cottonwood tree for a synthetic waveform footprint as a starting point. The modeled large-footprint lidar waveform is the sum of the reflections from different parts in the footprint that vertically stacked the elevations produced by the small-footprint elevation data. Fig. 3a contains the three-dimensional distribution of small-footprint lidar data from within a 26 m footprint centered on a tree approximately 30 m tall. Fig. 3b illustrates the distribution of these points as a function of height. A similar technique was used by Blair and Hofton (1999), which demonstrated that vertical distribution of the small-footprint lidar data is closely related to the full waveforms recorded by waveform-recording devices in tropical forests in Costa Rica. However, modeling of large-footprint return waveform in cottonwood riparian forests remains untested and any related analytical and processing issues are yet to be identified. As in Blair and Hofton's (1999) study, we tested the similarity between each modeled waveform and the return waveform from the ILRIS scanner using Pearson correlation, ρ, given by $\rho = S_{xy}/\sqrt{S_{xx}S_{yy}}$, where S_{xx}, S_{yy}, and S_{xy} are the variances and shared variance of the ILRIS and synthetic waveforms. The waveform comparison utilized 2004 airborne lidar and 2004 ground-based ILRIS data.

Fig. 4 plots five synthetic waveforms and corresponding ILRIS return waveforms. The results of comparison of the modeled waveform and the return waveform from ILRIS for old cottonwood trees are presented in Fig. 4a–c. In this case, the highest ρ was 0.73 between the modeled and ILRIS waveforms. Fig. 4d and e contains the waveforms comparing modeled and ILRIS for mature cottonwoods. The highest ρ value increased from 0.73 to 0.75 when mature cottonwoods were considered. Simple, single modal waveforms are typically returned from flat, unvegetated ground surfaces (Fig. 4a and e). The modeled and ILRIS waveforms from vegetated regions were multi-modal, each mode representing a vertically distinct, consolidated layer within the canopy.

Overall, the ground and airborne-based waveforms had a good degree of correlation. Although the modeled and ILRIS waveforms identify reflecting layers at the same elevations, the relative strengths of reflections from those layers varied; for instance, the modeled and ILRIS waveforms both detected a reflecting surface at

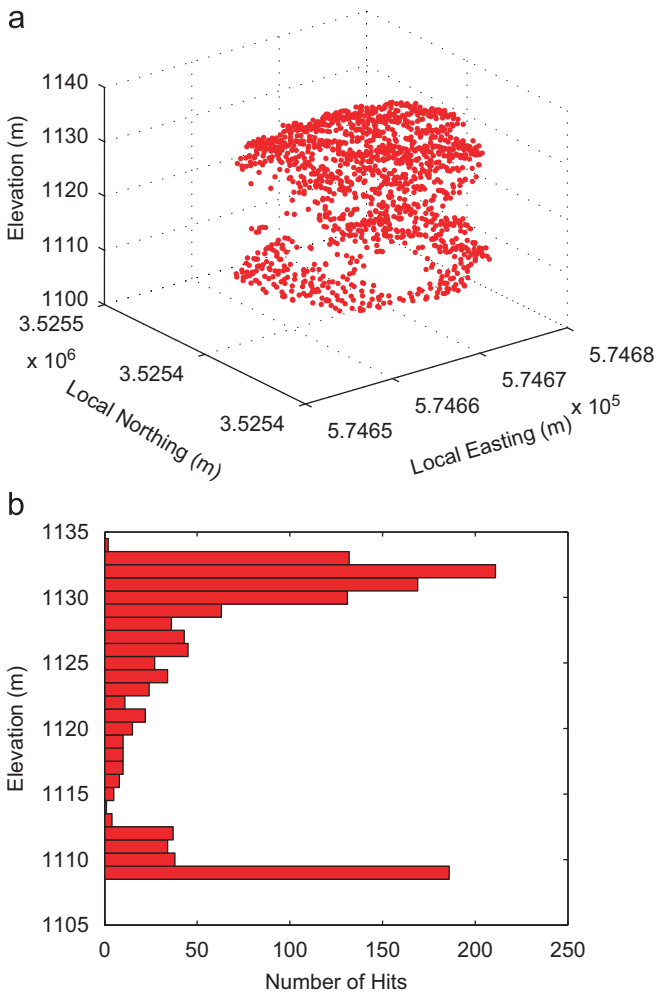

Fig. 3. Illustration of the potential for creating synthetic lidar waveforms from small-footprint lidar data. (a) shows the three-dimensional distribution of small-footprint lidar data from within a 22 m × 26 m footprint. (b) shows the vertical distribution of these returns.

~18 m elevation, but the reflection was much stronger when measured by ILRIS, possibly a result of different tree cover conditions at the time of the airborne and ILRIS surveys. The systematic difference noted between modeled and ILRIS waveforms was the consistently higher amplitude of the canopy response in the ILRIS return waveform (e.g. Fig. 4a). This difference is due to the first-return only nature of the ILRIS system, and a different view angle configuration between the airborne and ILRIS sensors. Also, a large gap through the canopy along the beam path may result in reduction of the amplitude of the canopy response in the modeled return waveform using the airborne system. Furthermore, the ILRIS system presents difficulties in detecting the uppermost portion of old cottonwood tree canopies because of the conical and flat-topped nature of the tree crown. However, the top portion of the crown may not be of sufficient area to register as a significant reflecting surface and therefore may not be detected well. Finally, the majority of modeled and ILRIS wave shapes have similar vertical structure in cottonwood trees.

4.2. Estimation of LAI from lidar data

4.2.1. The relationship between LAI and various laser height metrics

For each cottonwood tree, three laser height metrics were derived by all small-footprint lidar returns from the cottonwood canopy surface: (1) canopy height (h_{canopy}), (2) maximum laser height (Lz_{max}): the highest

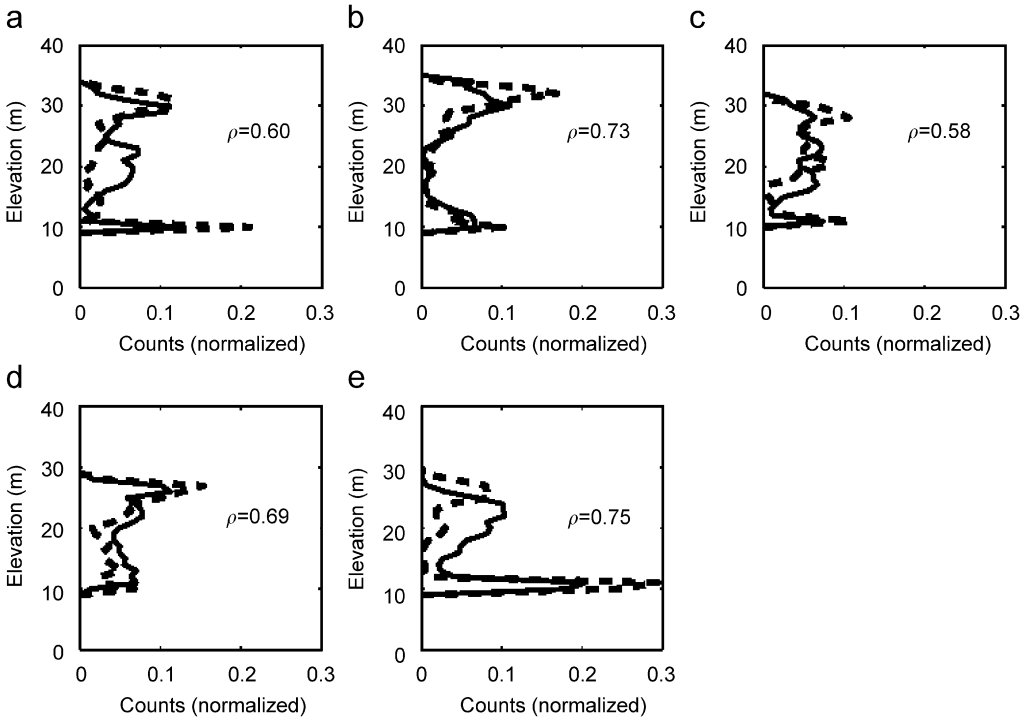

Fig. 4. ILRIS (solid line) and modeled (dashed line) waveforms for (a–c) old and (d–e) mature cottonwood trees. ρ is the Pearson correlation coefficient.

elevation of all lidar returns from canopy surface, and (3) mean laser height (Lz_{mean}): the mean laser elevation derived from all lidar returns for a canopy surface. To derive any type of tree height measurement, a ground reference level must be established. The point data in ground-classified hits were kriged to produce a Digital Elevation Model (DEM) with a 0.5 m pixel grid. The point data in vegetation-classified hits were interpolated to a regular grid that corresponded to the DEM, thereby creating a canopy altitude model. The canopy altitude model has a grid size of 0.5 m. Fig. 5 shows the terrain and overlaid canopy altitude model for the study site. The local maximum technique was used to discriminate cottonwoods in the canopy altitude model (Farid et al., 2006b). It operates with two shapes of the search window, specifically a square $n \times n$ window and a circular window that is more appropriate for identifying tree crowns. Variable window sizes were used by Wulder et al. (2000) for the extraction of tree locations and estimation of basal area from high spatial resolution imagery for stands of Douglas fir and western red cedar. The top of the tree was assumed to be the tallest point in the tree's canopy altitude model. The base of the tree was taken to be the point on the DEM beneath the top of the tree. Canopy height (h_{canopy}) was calculated by subtracting of the elevations of the bottom from the top of the tree.

Additionally, the derivation of two other laser height metrics is straightforward. The derivations of these two laser height metrics were formulated as Eqs. (1) and (2).

$$\text{Maximum laser height (m)} \quad Lz_{max} = \max(\text{all\_}z_{hits}\text{\_tree}), \tag{1}$$

$$\text{Mean laser height (m)} \quad Lz_{mean} = \frac{\sum_{i=1}^{n} \text{tree\_}z_{hit(i)}}{n}. \tag{2}$$

Fig. 6a–c contains the scatterplots comparing field-measured LAI and lidar-derived canopy height for each type of cottonwood tree. In this case, the coefficients of determination for field LAI versus lidar canopy heights were 0.77, 0.75, and 0.63 for young, mature, and old, respectively ($P<0.01$). As noted above, the lidar system presents difficulties in detecting the uppermost portion of old cottonwood tree canopies because of the conical nature of the tree crown and the small area of the top portion of the crown. In addition, determining

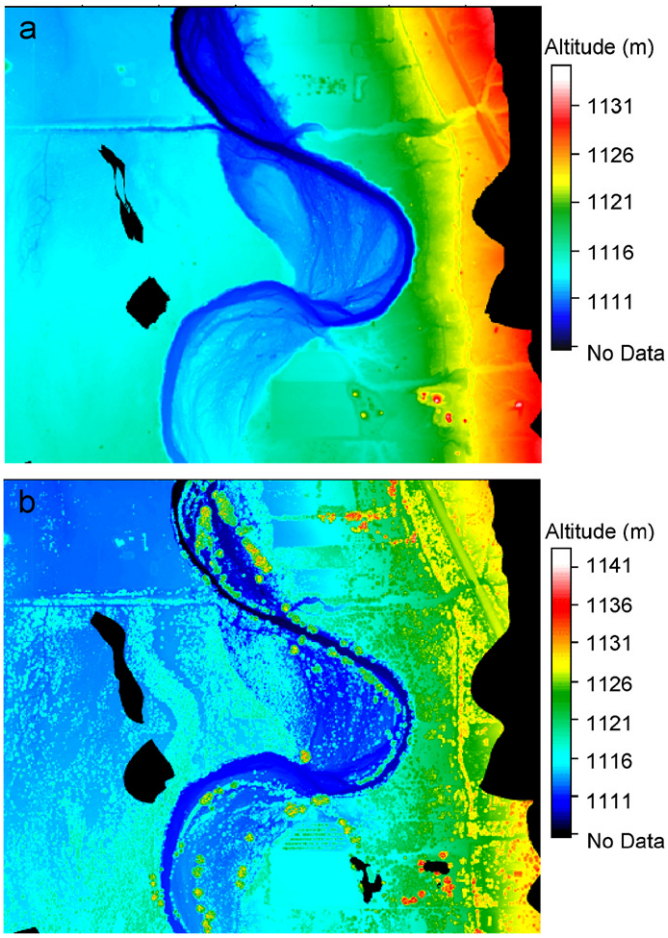

Fig. 5. Spatial pattern of DEMs (a) bare ground model and (b) canopy altitude model for the study site.

the exact elevation of the ground surface poses difficulties for both old and mature cottonwoods because the understory is dense enough to substantially occlude the ground surface. The r^2 increased from 0.63 to 0.77 when young cottonwoods were considered. The actual ground terrain detected by lidar for young trees is more accurate and precise than those estimates for old and mature trees because the area beneath the young trees is predominantly bare soil. The scatterplots comparing field-measured LAI and maximum laser height for each age class of cottonwood trees are presented in Fig. 6d–f. The coefficient of determination for field LAI versus maximum laser heights were 0.74, 0.73, and 0.67 for young, mature, and old, respectively ($P<0.01$). The lowest r^2 value was obtained for old cottonwoods for the reasons stated above.

The scatterplots comparing field-measured LAI and mean laser height for each age class of cottonwoods are shown in Fig. 6g–i. Results from regressing LAI and mean laser height on all age classes of cottonwoods did not produce r^2 values greater than 0.80, where the P-value was below the 0.05 significance level. Lz_{mean} is affected by canopy cover as demonstrated when Lz_{mean} was used to estimate LAI, where the mean laser height of an old cottonwood with high canopy cover was found to be dominated by the high number of laser returns from the canopy surface. The lowest r^2 value was obtained for young cottonwoods due to the presence of the gaps in young canopies which permitted a number of the laser pulses to penetrate the canopy, generating lower values for canopy cover. As a result, the Lz_{mean} value is problematic in a regression model.

4.2.2. *Estimation of LAI from synthetic lidar full waveforms*

Four metrics were derived by synthetically constructing a large-footprint lidar waveform (see Fig. 7) from the airborne small-footprint lidar data for different age classes of cottonwoods. Lidar canopy height (LHT)

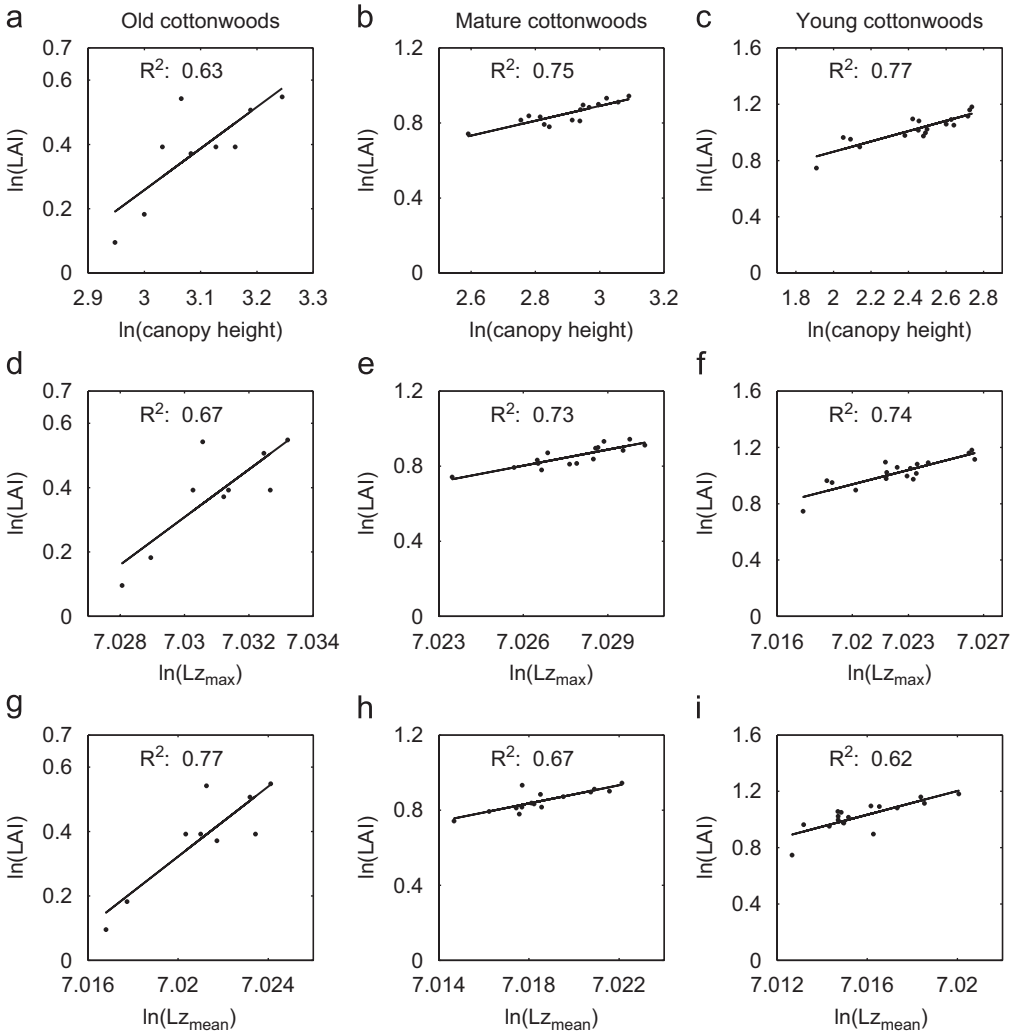

Fig. 6. Linear least-squares fit between LAI and (a–c) canopy height, (d–f) Lz_{max}, and (g–i) Lz_{mean} for each type of cottonwood tree on the study region.

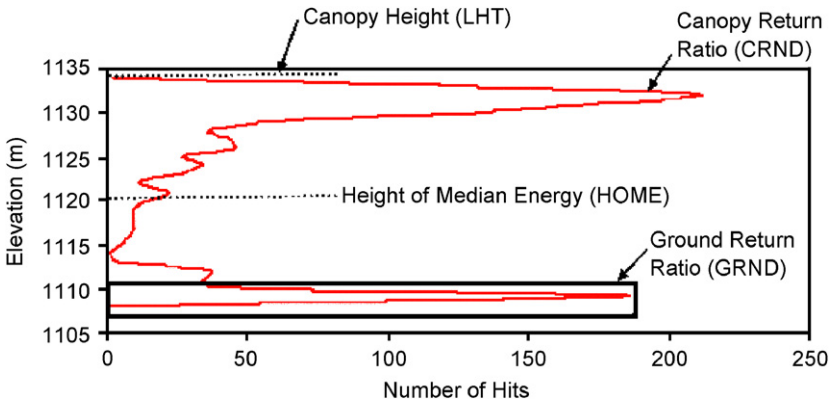

Fig. 7. Metrics derived from synthetic large-footprint lidar waveforms. See text for discussion. These metrics were then used to estimate LAI for different age classes of cottonwoods.

Table 1
Regression equations and statistics for relationship between LAI and lidar metrics for young, mature, and old-growth cottonwoods

Cottonwood age class	Equation	R^{2*}	RMSE	n
Young	Log (LAI) = 0.27 + 0.01*LHT + 0.01*HOME−0.01*GRND−0.02*CRND	0.76	0.02	17
Mature	Log (LAI) = 0.20 + 0.004*LHT + 0.02*HOME−0.01*GRND + 0.01*CRND	0.78	0.01	15
Old	Log (LAI) = −0.29−0.05*LHT + 0.16*HOME−0.47*GRND−0.83*CRND	0.84	0.04	9

*All values significant ($P<0.01$).

was calculated by identifying: (1) the location within the waveform when the first Gaussian pulse increased above a median energy level/threshold (the canopy top), and (2) the center of the last Gaussian pulse (the ground return), and then calculating the distance between these locations. Second, the HOME was calculated by finding the median of the entire waveform. The location of the median energy was then referenced to the center of the last Gaussian pulse to derive a height. The HOME metric is, therefore, predicted to be sensitive to changes in both the vertical arrangement of canopy elements and the degree of canopy openness (Drake et al., 2002). Third, a simple GRND was calculated by taking the number of hits in the last Gaussian peak divided by the sum of all other numbers of hits (total hits minus last Gaussian peak hits) (see Fig. 7). Thus, GRND provides an approximation of the degree of canopy closure (Drake et al., 2002; Means et al., 1999). Finally, the CRND was calculated by taking the number of hits in the location within the waveform when the first Gaussian pulse increases above a median energy level/threshold (the canopy top), divided by the sum of all other numbers of hits. CRND provides an approximation of the degree of canopy cover.

These four metrics were incorporated into a stepwise regression procedure to predict field-derived LAI for different age classes of cottonwoods. During this process, transformations of dependent and independent variables (including square, square root, and logarithmic) were also explored (Table 1). Metrics from the lidar waveform are able to estimate LAI for different age classes of cottonwood trees, though in all cases logarithmic transformation of the dependent variable was necessary. In this case, the coefficient of determination for field LAI versus lidar metrics were 0.76, 0.78, and 0.84 for young, mature, and old, respectively. Meanwhile, the RMSE for all age classes is low.

The weaker relationship between field LAI and lidar metrics in young trees could be affected by two factors. First, the level of variability in old tree structure at the scale of a waveform is higher than for a young one. A second contributing factor is the presence of gaps in young canopies, which allowed a number of the laser pulses to penetrate the canopy, generating lower values for CRND.

Also, in areas with densely packed canopy materials such as old canopies, fewer lidar pulses will reach the ground, thereby increasing HOME. Conversely, in more open or disturbed areas (e.g., a young tree canopy), more lidar pulses will reach the ground, reducing HOME. Additionally, the height metrics (e.g., LHT and HOME) are the most sensitive, and increase with increasing cottonwood tree age and basal area. The LHT is perhaps the metric with the strongest potential for estimating riparian forest structural characteristics. The LHT metric is influenced by the highest detectable canopy surface within a footprint.

Overall, we presented two approaches to predict field-derived LAI for different age classes of cottonwood trees. The first method used three laser height metrics (h_{canopy}, Lz_{max}, and Lz_{mean}), which were derived from small-footprint lidar returns (see Fig. 6). The second method used four metrics (LHT, HOME, GRND, and CRND) that were derived by synthetic construction of a large-footprint lidar waveform from the airborne small-footprint lidar data (see Fig. 7). The comparison between these methods showed that much effort and more time are needed to derive synthetic large-footprint lidar waveform, and it is apparent that extra cost will be required for this task.

4.3. Estimation of cottonwood transpiration from lidar data

In this section, we present the lidar-predicted versus sap flow measured cottonwood transpirations at two contrasting riparian sites in order to more accurately estimate cottonwood water use. Along the San Pedro River, Gazal et al. (2006) quantified cottonwood transpiration using sap flow measurements for an isolated

cluster of trees located on a perennial section of the river and another located along a reach with intermittent stream flow. Hydrologically, these sites differed in the depth and seasonal fluctuation of the water table.

The P–M model (Monteith and Unsworth, 1990) was selected to estimate cottonwood transpiration using lidar-derived LAI for June 1 through June 11, 2003 (DOY: 152–162). This model allows the calculation of evaporation from meteorological variables and resistances which are related to the stomatal and aerodynamic characteristics of the tree, and has the form

$$E = \frac{1}{\lambda}\left[\frac{\Delta A + \rho_a c_p D/r_a}{\Delta + \gamma(1 + r_c/r_a)}\right] \text{(mm/day)}, \tag{3}$$

where Δ is the slope of the saturation vapor pressure/temperature curve (kPa $^{\circ}C^{-1}$), ρ_a the density of moist air (kg m^{-3}), $c_p = 1.013$ (kJ kg^{-1} $^{\circ}C^{-1}$) the specific heat capacity of dry air under constant pressure, D the vapor pressure deficit (kPa), γ the psychrometric constant (kPa $^{\circ}C^{-1}$), r_c the bulk canopy resistance (s m^{-1}), r_a the aerodynamic resistance (s m^{-1}), λ the latent heat of vaporization of water (MJ kg^{-1}), and A the available energy (MJ m^{-2} day^{-1}). Parameters such as Δ, ρ_a, γ, and D were calculated from air temperature, relative humidity, and air pressure measured from nearby meteorological stations. The available energy to the canopy is given by

$$A = S\downarrow(1 - \alpha) + L_{net} - S_t, \tag{4}$$

where S is the incoming solar radiation (MJ m^{-2} day^{-1}), α the canopy albedo, L_{net} the net long-wave radiation (MJ m^{-2} day^{-1}), and S_t the temporary storage of energy into the tree itself (trunk and limbs) and the energy used in the photosynthesis process (MJ m^{-2} day^{-1}). Canopy albedo was estimated to be 0.18, a value which has been measured over broadleaf oak trees (Bras, 1990). S_t was estimated to be 5% of the incoming solar radiation based on work by Moore and Fisch (1986) who found that S_t ranged between 0% and 10% of the net radiation available to a tropical forest. The net long-wave radiation contribution to the available energy was calculated from a formula provided by Shuttleworth (1993, p. 4.7).

The aerodynamic resistance (r_a) is the sum of the turbulent resistance between the canopy and the atmosphere from turbulent eddies and the boundary layer resistance (Thom, 1975). Due to the relatively open nature of the cottonwood canopy, the turbulent canopy resistance is assumed negligible in comparison to the boundary layer resistance (Goodrich et al., 2000). Hence r_a is assumed to equal the boundary layer resistance (r_b). To estimate the boundary layer resistance, the model proposed by Choudhury and Monteith (1988) was used:

$$r_b = \frac{1}{(\text{LAI})(b)}\frac{\alpha_{att}}{(1 - \exp(-(1/2)\alpha_{att}))}\sqrt{\frac{\omega}{U}}. \tag{5}$$

In this equation, LAI is the canopy projected Leaf Area Index (the same as Leaf Area Index) derived from synthetic large-footprint lidar. The quantity b was set equal to 0.0067 m s$^{-1/2}$. It is a scaling coefficient for leaf boundary layer resistance (Magnani et al., 1998). α_{att} is an attenuation coefficient for wind speed inside the canopy, $\omega = 0.05$ m is a typical leaf width, and U the wind speed outside the canopy (measured at 10 m above the ground). The value for the wind attenuation coefficient, α_{att}, was set equal to 3 following Magnani et al. (1998).

The only remaining quantity required to compute cottonwood transpiration is the bulk canopy resistance (r_c). The canopy resistance is related to individual leaf stomatal resistance (r_s) by the following expression (Goodrich et al., 2000):

$$r_c = \frac{r_s}{2\text{LAI}}, \tag{6}$$

where r_s was estimated by Gazal et al. (2006) at both sites. LAI was derived for both sites using the modeled waveform lidar and from ground-based measurements (LAI 2000, Li-Cor, Inc., Lincoln, NE; Gazal et al., 2006). The lidar-derived LAI at the perennial was 3.48 and at intermittent stream site was 2.78. It was assumed that these values were constant over the study period (DOY: 152-162) centered around the lidar flight.

Daily total lidar-predicted transpiration of the cottonwoods at the perennial stream site was higher than that at the intermittent stream site throughout the study period (Fig. 8). Total lidar-predicted E was 23 mm at

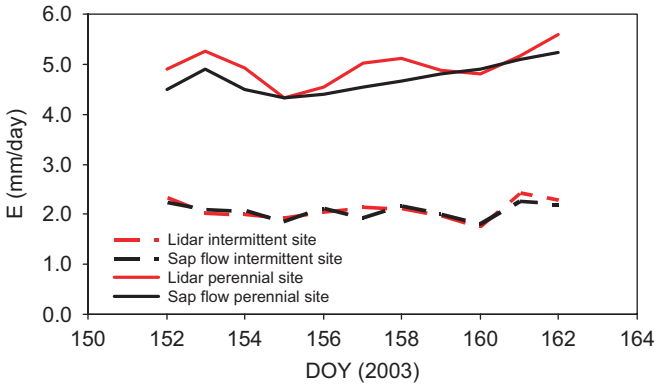

Fig. 8. Daily total lidar-predicted versus sap flow measured cottonwood transpirations at the intermittent and perennial stream sites.

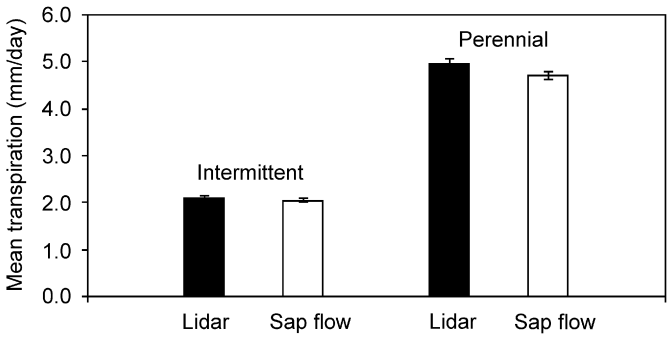

Fig. 9. The lidar-predicted versus sap flow measured cottonwood mean daily transpirations at the intermittent and perennial stream sites over an 11-day period centered on the lidar flight.

the intermittent stream site, and 55 mm at the perennial stream site. This is consistent with Schaeffer et al. (2000) who found that riparian water use was correlated to LAI. Depth to groundwater (d_{gw}) at the intermittent stream site was deeper than at the perennial stream site. At the intermittent stream site, d_{gw} increased from 3.1 m during the early part of the spring season to 3.9 m during the peak of the drought period (Gazal et al., 2006). At the perennial stream site, d_{gw} had a gradual but much smaller decline during the pre-monsoon drought. The depth at the beginning of the spring season was 1.5 m and increased to only 1.8 m at the peak of the drought period (0.5 m less than at the intermittent site; Gazal et al., 2006). Thus, greater depths to groundwater corresponded with lower rates of lidar-predicted LAI and transpiration. Additionally, r_s at the intermittent stream site was greater than at the perennial stream site with maximum r_s attained at the peak of the pre-monsoon drought period (Gazal et al., 2006). At the intermittent stream site, the combination of decreased LAI and the increase in r_s caused large reductions in lidar-predicted transpiration that may be associated with both loss of leaf area and the loss of hydraulic conductivity that also facilitated a reduction in stomatal conductance.

Lidar-predicted transpiration of the cottonwoods at two stream sites was 2–5% more than their sap flow measurements (Fig. 9). The differences in lidar-derived LAI and ground-based measurements of LAI (LAI 2000, Li-Cor, Inc., Lincoln, NE; Gazal et al., 2006) account for most of the differences in the magnitude of E. Lidar-derived LAI was greater than ground-based measured LAI at two stream sites. Hence, greater LAI values corresponded with higher rates of cottonwood transpiration at two contrasting riparian sites.

5. Conclusions

We have shown that one can synthesize the vertical structure information for cottonwood trees in a medium-large footprint laser altimeter return waveform using a small-footprint elevation data set. The

similarity between modeled waveform and return waveform from ILRIS scanner was assessed using the Pearson correlation statistic. Overall, the waveforms had a good degree of correlation. Although the modeled and ILRIS waveforms identify reflecting layers at the same elevations, the relative strengths of reflections from those layers varied. In addition, cottonwood tree-age changes are likely mirrored in the shape or vertical geolocation of the waveform.

For each cottonwood tree, three laser height metrics were derived by all small-footprint lidar returns from cottonwood canopy surface. The h_{canopy} and Lz_{max} laser height metrics were demonstrated as capable of estimating LAI for different age classes of cottonwoods. Additionally, four metrics were derived from the modeled large-footprint return waveforms for different age classes of cottonwood trees in a riparian corridor. These four metrics were incorporated into a stepwise regression procedure to predict field-derived LAI. The metrics from the lidar waveform were able to estimate LAI for different age classes of cottonwood trees, though in all cases logarithmic transformation of the dependent variable was necessary.

Lidar and meteorological-based estimates of cottonwood transpiration versus sap flow estimated transpiration at perennial and intermittent riparian sites were also made. Lidar-met-based transpiration estimates of the cottonwood at the two stream sites were 2–5% greater than their sap flow measurements over an 11-day period centered on the lidar flight. The differences in lidar-derived LAI and ground-based measurements of LAI account for most of the differences in the magnitude of E.

Overall, airborne lidar offers the distinct advantage of providing LAI estimates over large areas which can then be used to improve riparian water-use estimates. Airborne, multi-return small-footprint lidar systems are becoming more widely available and the cost of lidar data acquisition is expected to continue to decrease. This study primarily concentrated on individual cottonwood trees to develop the relationships to estimate LAI for riparian water-use estimates and may not be applicable to dense, overlapping canopies. Additionally, lidar cannot provide information on stomatal control which also regulates riparian cottonwood water use so independent estimates or typical ranges of canopy-level stomatal resistance will be required. However, strategically acquired lidar data and derived spatially explicit LAI measurements offer significant potential to improve corridor-level riparian water-use estimates.

Future research will investigate how well lidar can derive LAI in more complex and interacting canopies at the overall corridor level. The P–M model to estimate cottonwood transpiration using lidar-derived canopy metrics for the whole riparian corridor will then be investigated.

Acknowledgments

This study is based upon work supported by SAHRA (Sustainability of semi-Arid Hydrology and Riparian Areas) under the STC Program of the National Science Foundation, Agreement No. EAR-9876800. Funds provided by the U.S. Dept. of Defense Legacy Program in support of this research are gratefully acknowledged. We are indebted to the following people who assisted us in various aspects of this work: Michael Sartori and William Cable. In addition, we wish to acknowledge the staff at the USDA-ARS Southwest Watershed Research Center, Tucson, Arizona.

References

Abshire, J.B., McGarry, J.F., Pacini, L.K., Blair, J.B., Elman, G.C., 1994. Laser altimetry simulator version 3.0 user's guide, NASA Technical Memorandum 104588, Greenbelt, Maryland, p. 70.

Blair, J.B., Hofton, M.A., 1999. Modeling laser altimeter return waveforms over complex vegetation using high-resolution elevation data. Geophysical Research Letters 26, 2509–2512.

Bras, R., 1990. Hydrology. Addison-Wesley, Reading, MA, p. 44.

Choudhury, B.J., Monteith, J.L., 1988. A four-layer model for the heat budget of homogeneous land surfaces. Quarterly Journal of Royal Meteorological Society 114, 373–398.

Drake, J.B., Dubayah, R.O., Clark, D.B., Knox, R.G., Blair, J.B., Hofton, M.A., Chazdon, R.L., Weishampel, J.F., Prince, S.D., 2002. Estimation of tropical forest structural characteristics using large-footprint lidar. Remote Sensing of Environment 79, 305–319.

Farid, A., Rautenkranz, D., Goodrich, D.C., Marsh, S.E., Sorooshian, S., 2006a. Riparian vegetation classification from airborne laser scanning data with an emphasis on cottonwood trees. Canadian Journal of Remote Sensing 32, 15–18.

Farid, A., Goodrich, D.C., Sorooshian, S., 2006b. Using airborne lidar to discern age classes of cottonwood trees in a riparian area. Western Journal of Applied Forestry 21, 149–158.

Gardner, C.S., 1992. Ranging performance of satellite laser altimeters. IEEE Transactions on Geoscience and Remote Sensing 30, 1061–1072.

Gazal, R.M., Scott, R.S., Goodrich, D.C., Williams, D.G., 2006. Controls on transpiration in a semiarid riparian cottonwood forest. Agricultural and Forest Meteorology 137, 56–67.

Goodrich, D.C., Scott, R., Qi, J., Goff, B., Unkrich, C.L., Moran, M.S., Williams, D., Schaeffer, S., Snyder, K., Macnish, R., Maddock, T., Pool, D., Chehbouni, A., Cooper, D.I., Eichinger, W.E., Shuttleworth, W.J., Kerr, Y., Marsett, R., Ni, W., 2000. Seasonal estimates of riparian evapotranspiration using remote and in-situ measurements. Agricultural and Forest Meteorology 105, 281–309.

Maclean, G.A., Krabill, W.B., 1986. Gross-merchantable timber volume estimation using an airborne LIDAR system. Canadian Journal of Remote Sensing 12, 7–18.

Magnani, F., Leonardi, S., Tognetti, R., Grace, J., Borghetti, M., 1998. Modelling the surface conductance of a broadleaf canopy: effects of partial decoupling from the atmosphere. Plant, Cell Environment 21, 867–879.

Means, J.E., 2000. Comparison of large-footprint and small-footprint lidar systems: design, capabilities, and uses. In: Proceedings of the Second International Conference on Geospatial Information in Agriculture and Forestry. Lake Buena Vista, Florida, pp. 85–192.

Means, J.E., Acker, S.A., Harding, D.J., Blair, J.B., Lefsky, M.A., Cohen, W.B., Harmon, M., McKee, W.A., 1999. Use of large-footprint scanning airborne lidar to estimate forest stand characteristics in the western Cascades of Oregon. Remote Sensing of Environment 67, 298–308.

Monteith, J.L., Unsworth, M.H., 1990. Principles of Environmental Physics. Edward Arnold, London, England.

Moore, C.J., Fisch, G., 1986. Estimating heat storage in Amazonian tropical forests. Agricultural and Forest Meteorology 38, 147–169.

Nelson, R.F., Krabill, W.B., Maclean, G.A., 1984. Determining forest canopy characteristics using airborne laser data. Remote Sensing of Environment 15, 201–212.

Nelson, R.F., Swift, R., Krabill, W.B., 1988a. Using airborne lasers to estimate forest canopy and stand characteristics. Journal of Forestry 86, 31–38.

Nelson, R.F., Krabill, W.B., Tonelli, J., 1988b. Estimating forest biomass and volume using airborne laser data. Remote Sensing of Environment 24, 247–267.

Schaeffer, S.M., Williams, D.G., Goodrich, D.C., 2000. Transpiration of cottonwood/willow forest estimated from sap flux. Agricultural and Forest Meteorology 105, 257–270.

Scott, R.L., Shuttleworth, W.J., Goodrich, D.C., Maddock III, T., 2000. The water use of two dominant vegetation communities in a semiarid riparian ecosystem. Agricultural and Forest Meteorology 105, 241–256.

Shuttleworth, W.J., 1993. Evaporation. In: Maidment, D.R. (Ed.), Handbook of Hydrology. McGraw-Hill, New York, pp. 4.1–4.53.

Stromberg, J.C., 1998. Dynamics of Fremont cottonwood (*Populus fremontii*) and saltcedar (*Tamarix chinensis*) populations along the San Pedro River, Arizona. Journal of Arid Environments 40, 133–155.

Thom, A.S., 1975. Momentum, mass and heat exchange of plant communities. In: Monteith, J.L. (Ed.), Vegetation and the Atmosphere. Academic Press, New York, pp. 57–109.

US Department of the Interior, 2006. Water management of the regional aquifer in the Sierra Vista sub watershed, Arizona—Report to Congress. US Geological Survey, 26.

Wehr, A., Lohr, U., 1999. Airborne laser scanning—an introduction and overview. ISPRS Journal of Photogrammetry and Remote Sensing 54, 68–82.

World Rivers Review, 1997. Biodiversity, North America. World Rivers Review, News Briefs 12, February 1997. International Rivers Network, Internet document 〈http://www.irn.org/pubs/wrr/9701/briefs.html〉 (last date accessed: 15 May 2004).

Wulder, M., Niemann, K.O., Goodenough, D.G., 2000. Local maximum filtering for the extraction of tree locations and basal area from high spatial resolution imagery. Remote Sensing of Environment 73, 103–114.